



# Modeling and optimization for selecting LED to synthesize solar spectrum using residual-guided evolution algorithms

Qingguang Chen\*, Xing Jin, Lingyun Xue

Hangzhou Dianzi University, College of life information and instrumentation engineering, 2nd Street of Xiasha High Education Zone, Hangzhou, 310018, China

## ARTICLE INFO

### Keywords:

Solar spectrum synthesis  
LED type selection  
SMREA  
SPD modeling  
Differential evolution (DE) algorithm

## ABSTRACT

LED has proven to be promising artificial light source to match solar spectrum in photovoltaic field. Selection of LED type from product database and working parameters determination for each type LED are essential problems to be solved. In this paper, a spectral match residual-guided evolution algorithm (SMREA) was proposed to solve the problems. Dependence of spectral match and correlation index of synthesized spectrum on LED type number are investigated from our LED type database. The results reveal that spectral synthesis performance dramatically improves firstly with increasing LED type number and after combination reached a certain number, it begins to stabilize. In our study, 4 types of LED can achieve spectral match deviation 21.45% in range of 400 nm–800 nm with low correlation index 0.7606. When the number of LED types added to 7, 11, and 13, the spectral match deviation can decreased to be 5.94%, 2.65%, 3.65% respectively and the correlation index increases to be 0.9039, 0.9691, 0.9841. SMREA can also output working parameters of LED at corresponding evolved type number. The feasibility of SMREA to solve the dual optimization problem was effectively validated. The reported work provides a significant value for LED type selection of LED-based solar spectral synthesis.

## 1. Introduction

Solar simulator is an indispensable tool in photovoltaic field for characterization test, developing and quality control of solar cell [1]. As a controllable indoor test facility, it can provide near real sunlight spectrum under laboratory conditions using artificial light source such as quartz-tungsten halogen lamps, mercury xenon lamps, xenon arc, xenon flash lamps, metal halide lamps, LED and so on [2]. Xenon lamp, as the mostly common traditional light source used currently, utilizes air mass filters to reshape the radiation spectral distribution for good agreement with solar spectrum [3]. But radiant flux output range is difficult to electrically control due to the limitation of operational principal of high-pressure ionization lighting. To obtain radiant flux at different levels, neutral density filters were generally used for intensity reduction [4]. Obviously, filter-based adjustable radiant flux output of Xenon lamp is difficult and expensive to maintenance. As a new solid state lighting artificial source, LEDs have shown great promise as alternative light source for solar simulator for its excellent technical features superior to traditional light source. The commercial availability of wide variety of colors from ultraviolet to infrared and relative narrow-band monochromatic output spectrum make it possible for spectral superposition to create a close-match AM1.5G solar spectrum by combination of multiple LEDs with various types. Additionally, individual regulation of LED over a wide intensity range allows achievement of adjustable radiant flux output. Moreover, characteristics of high optical power, long lifetimes, compactness and energy saving, etc provide much greater flexibility in design and

\* Corresponding author.

E-mail address: [optichen@hdu.edu.cn](mailto:optichen@hdu.edu.cn) (Q. Chen).

<https://doi.org/10.1016/j.ijleo.2018.12.134>

Received 7 December 2018; Accepted 26 December 2018

0030-4026/ © 2018 Elsevier GmbH. All rights reserved.

implementation of LED-based solar simulator [5,6]. LED has been considered to redefine photovoltaic device characterization [7].

LED has attracted great attentions to synthesize solar spectrum. In the early stage, the possibility of creating a close-match AM1.5 G spectrum by combination a number of different types of LED was evaluated [8,9]. Then amounts of solutions have then been proposed to validate the feasibility of LED-based solar spectral synthesis. It has been reported that LEDs of 8 different types covering 375 nm–680 nm combined with halogen lights supplementing infrared spectrum were used to investigate solar spectrum synthesis. In the LED-contributed spectral range of 400 nm–700 nm, class A spectral match has been achieved [10,11]. After that, fully LED-based designing scheme for solar spectral synthesis continuously appears. High-power LED with 18 different types covering wavelength range of 390–940 nm have been used to develop solar cell test platform [12]. Class A solar spectral match in wavelength range of 350 nm–800 nm have been proven using only six LED colors [13]. Accurate solar spectrum match solution with better than Class A level is proposed by 26 different types to minimize the spectral mismatch and improve measurement uncertainty, [14]. Meanwhile, class A spectral match compactly achieved by six high-power types of LEDs has also been reported [15,16]. With 11 different LED types, class A + AM1.5 g spectrum between 400 and 750 nm has been experimental achieved [17].

Due to wide range of class A spectral match defined by IEC standard, aforementioned literatures indicate that different LED types combination all can fulfill requirement of class A spectral match. LED type selection from variety of commercial products is an essential problem for LED-based spectral synthesis to achieve the desired solar spectrum, and the selection result will influence design complexity, optical performance, manufacturing cost and physical size, etc.. LED combination solutions used in the reported application lacking rational selection rules might not be optimal for solar spectral synthesis.

There already have a few researches on LED type selection method for multi-LED spectral synthesis. Empirical method was proposed to select high-power LED type in each of the six wavelength ranges defined for performance evaluation of AM1.5 G solar simulator [16]. Obviously, the selection method has disadvantage of randomness as well as varieties. LED type selection belongs to multi-parameters combination optimization. Therefore, genetic algorithm was used to choose combination of LEDs for each iteration [14]. The pruning process was proposed by removing LEDs from the candidate LED set containing a large number of available LEDs to minimize synthesis error [18,19]. Subtraction operation by removing LED type contributing the least to the combination from the original group was experimentally conducted to find the optimal combination [20]. Obviously, subtraction-based method cannot assure the global optimization result.

On the basis of LED type selection, contribution of each type is necessary to determine for synthesizing solar spectrum with specific radiant flux. Number and driving current are the direct control parameters. The past studies generally search number of SPD at rated forward current to synthesize solar spectrum [14,15]. Parameter search space is not continuous and it failed to make full use of LED of easy electrically control of SPD. Obviously, taking number and current into consideration shall be helpful to improve spectral synthesis.

According to standard IEC 60904-9, spectral match is one of the evaluation indexes of illumination source used for solar cell parameter measurement, which is defined as the ratio of the actual percentage of irradiance falling on the interval of concern and the required percentage of irradiance. Class A level is rated as the fraction within  $\pm 25\%$  deviation, which is a wide range. For solar cell performance measurement, spectral mismatch factor caused by spectral deviation of synthesized light sources from standard spectrum is introduced to correct measurement error [21]. Research shows that light sources with the same Class A level has significantly different spectral mismatch error [22]. Therefore, nearly perfect match of AM1.5 G spectrum is the goal for accurate measurement.

In this paper, dual optimization problem of type selection and working parameter determination was described for LED-based spectral synthesis. One kind of heuristic optimization approach for LED type selection named spectral match residual-guided evolution algorithm (SMREA) was proposed and detailed realization was illustrated. The dependence of type selection and spectral synthesis performance was analyzed and discussed. The working parameters of number and current of each type were also given for different spectral performance.

## 2. Problem formulation

Multi-types LED-based solar spectral synthesis can be considered as superposition results of multiple LEDs with different SPDs and different numbers. The mathematical principle can be described in Eq. (1).

$$\Phi(\lambda) = \sum_{i=1}^k N_i S_i(\lambda, I_i) \quad (1)$$

$\Phi(\lambda)$  in the formula is the targeted solar spectral power distribution.  $k$  is LED type numbers,  $N_i$  is the number of  $i$ th type LED, and  $S_i(\lambda, I_i)$  is spectral power distribution of  $i$ th type LED at driving current  $I_i$ . Obviously, type selection from existing commercial products and determination of working parameters of number and driving current for each type LED are problems necessary to be identified, which is a complex dual optimization problem.

The first optimization aim is to find the minimum type numbers of LED combination to meet AM1.5 G solar spectral matching requirements which can be illustrated as:

$$\begin{aligned} & \arg \min_{\text{types} \in \Omega} k \\ & \text{s. t. } SM \leq T_{SM}, k \leq N_{total} \end{aligned} \quad (2)$$

where  $\Omega$  denotes LED type set collected from market, and the total number is  $N_{total}$ ,  $k$  is number of selected LED type,  $SM$  is the

spectral mismatch using  $k$  types LED combination,  $T_{SM}$  is targeted spectral mismatch value.

The followed optimization is to determine working parameters of each type LED for spectral synthesis to best match solar spectrum allowing for desired spectral mismatch under selected  $k$  LED types combination. The formulated optimized problem is shown in Eq. (3).

$$\begin{aligned} \arg \min f(N_1, N_2, \dots, N_k, I_1, I_2, \dots, I_k) &= \alpha e_{sse} + (1 - \alpha) e_{var} \\ \text{s. t. } I_{j,\min} &\leq I_j \leq I_{j,\max} \quad 1 \leq N_j \leq N_{j,\max} \quad j = 1, 2, \dots, k \end{aligned} \quad (3)$$

where  $e_{sse}$  denotes sum of squared error,  $e_{var}$  indicates error distribution variance used to evaluate uniformity of spectral match error distribution for  $n$  wavelength bands and minimized variance can improve accuracy of spectral mismatch correction factor.  $\alpha$  is scale coefficient ranging  $[0, 1]$ , which determines objective function tended to error value or uniformity of error distribution.  $[I_{j,\min}, I_{j,\max}]$ ,  $[1, N_{j,\max}]$  are constrained range of forward current and number for each type LED. And  $e_{var}$ ,  $e_i$  are defined as:

$$e_{sse} = \sum_{\lambda=\lambda_{\min}}^{\lambda_{\max}} \left( \sum_{j=1}^k N_j S_j(\lambda, I_j) - \Phi(\lambda) \right)^2 \quad (4)$$

$$e_{var} = \sum_{i=1}^n (e_i - \bar{e})^2 / n \quad (5)$$

where  $e_i = \sum_{\lambda=\lambda_i}^{\lambda_i+\Delta\lambda_i} \left( \sum_{j=1}^k N_j S_j(\lambda, I_j) - \Phi(\lambda) \right)^2$  is the spectral match error for  $i$ th wavelength band in the range  $[\lambda_i, \lambda_i + \Delta\lambda_i]$ ,  $\bar{e} = \sum_{i=1}^n e_i / n$  is average error.

The above-mentioned optimization problems have mutual influence on each other and cannot be solved analytically. Therefore, advanced optimization algorithm is needed to be introduced to obtain an optimized solution.

### 3. Residual-guided evolution algorithm

For design of multiple LED-based AM1.5 G solar spectral synthesis application, spectral match deviation in each wavelength band defined in standard needs to be less than target  $T_{sm}$ . Increasing number of LED types will generally improve spectral match. Analyzing spectral match residual distribution at different wavelength band gives guidance for selecting and adding LED type. Therefore, spectral match residual-guided evolution algorithm (SMREA) for LED types selection is proposed in the paper to investigate the dependence of spectral match on types number of LED and determine the working parameter of each type LED for dual optimization problem. The detailed implementation of SMREA for LED type selection is shown as a flowchart in Fig. 1.

As can be seen from the flowchart, it involves different steps that are explained as follows.

Step 1: Initialization of parameters.

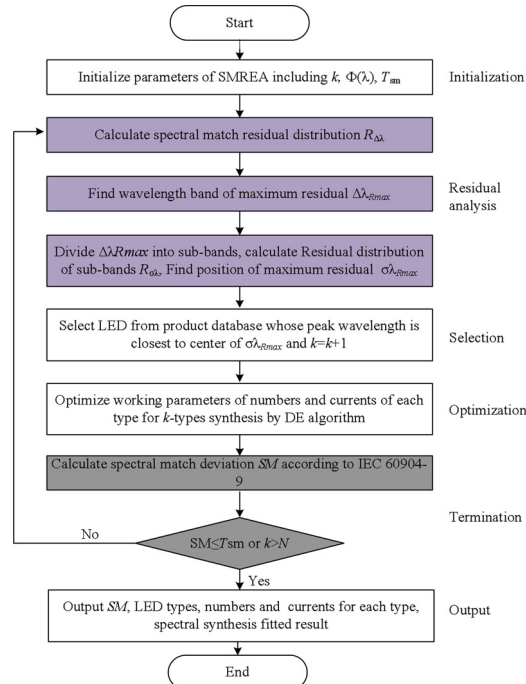


Fig. 1. Flowchart of SMREA for LED types selection of solar spectrum synthesis.

Target of spectral match deviation  $T_{sm}$ , SPD of AM1.5 G at required radiant flux level  $\Phi(\lambda)$ , number of LED type  $k=0$  are initialized. Spectral range is divided to four wavelength bands with spectral interval  $\Delta\lambda = 100$  nm according to evaluation parameter defined in IEC standard 60904-9.

Step 2: Residual analysis.

Spectral match residual  $R_{\lambda_i, \Delta\lambda}$  is defined as Eq. (6) for wavelength band  $(\lambda_i, \lambda_i + \Delta\lambda)$ .

$$R_{\lambda_i, \Delta\lambda} = \left| 1 - \frac{\sum_{\lambda=\lambda_i}^{\lambda_i+\Delta\lambda} S_f(\lambda) / \sum_{\lambda=\lambda_{min}}^{\lambda_{max}} S_f(\lambda)}{\sum_{\lambda=\lambda_i}^{\lambda_i+\Delta\lambda} \Phi(\lambda) / \sum_{\lambda=\lambda_{min}}^{\lambda_{max}} \Phi(\lambda)} \right| \quad (6)$$

where  $S_f(\lambda) = \sum_{i=1}^k N_i S_i(\lambda, I_i)$  is the fitted spectral synthesis result.  $N_i, I_i$  are working parameters of number and driving current respectively for  $i$ th type LED.  $k$  is the number of selected LED types.  $\Phi(\lambda)$  is targeted spectrum.  $\lambda_{min}, \lambda_{max}$  are the lower and upper limit of considered spectral range.

Therefore, spectral match residual distribution  $R_{\Delta\lambda} = (R_{\lambda_1, \Delta\lambda}, R_{\lambda_2, \Delta\lambda}, \dots, R_{\lambda_n, \Delta\lambda})$  can be obtained and the wavelength band of maximum residual  $\Delta\lambda_{Rmax}$  can be determined.

Step 3: Selection of LED type for adding.

To select LED type from product database,  $\Delta\lambda_{Rmax}$  is divided by wavelength interval  $\sigma\lambda$  into multiple sub-bands. Then spectral match residual distribution of sub-bands  $R_{\delta\lambda} = (R_{\delta\lambda_1}, R_{\delta\lambda_2}, \dots, R_{\delta\lambda_n})$  can be calculated by formula defined in Eq. (2). Maximum residual position in sub-bands  $\sigma\lambda_{Rmax}$  can then be obtained. LED type from product database whose peak wavelength is closest to center of  $\sigma\lambda_{Rmax}$  is then selected and  $k$  is then set as  $k = k + 1$ .

Step4: Optimization of working parameters for each type of LEDs

Differential evolution algorithm (DEA) is a population-based stochastic heuristic searching algorithm suitable for solving optimization problems [23,24]. Solar spectral synthesis using  $k$  types LED represented in Eq. (3) can be optimized by DEA to obtain working parameters of corresponding numbers and driving currents under constraint conditions. DEA includes four steps: initialization, mutation, crossover, and selection operations. The detailed implementation can be found in the following.

Step 4.1: Initialization of parameter vectors.

Randomly population including  $N_p$   $2k$ -dimension parameter vectors is initialized as the candidate solution. The  $i$ th parameter vector of the population can be represented as:

$$x_i^{(g)} = (N_{i,1}^{(g)}, N_{i,2}^{(g)} \dots N_{i,k}^{(g)}, I_{i,1}^{(g)}, I_{i,2}^{(g)}, \dots, I_{i,k}^{(g)}) \quad (7)$$

where  $N_{i,j}^{(g)}, I_{i,j}^{(g)}$  are the number and current of  $j$ th type LED respectively at the  $g$ th generation. The  $j$ th component of  $i$ th parameter vector is randomly initialized in the constrained number range  $[N_{j,min}, N_{j,max}]$  and current working range  $[I_{j,min}, I_{j,max}]$ .

Step 4.2: Mutation with difference vectors.

Differential mutation operation is used to extend search space in DE. Donor vector  $V_i^{(g)}$  can be obtained by mutation strategy expressed in Eq. (8).

$$V_i^{(g)} = x_{best}^{(g)} + F(x_{R_1}^{(g)} - x_{R_2}^{(g)}) \quad (8)$$

where  $x_{best}^{(g)}$  is the best individual parameter vector with the best fitness value according to the objective function defined in Step 4.4 in the population at iteration  $g$ .  $R_1, R_2$  are mutually exclusive integers randomly chosen from the range  $[1, N_p]$ , therefore, target vector  $x_{R_1}^{(g)}$  and  $x_{R_2}^{(g)}$  can be selected.  $F$  is positive scaling factor for scaling the difference vectors.

Step 4.3: Crossover.

Crossover operation mixes component of donor vector  $V_i^{(g)}$  with the target vector  $x_i^{(g)}$  to form the trial vector  $U_i^{(g)}$ . The binomial scheme used can be expressed as:

$$U_{i,j}^{(g)} = \begin{cases} V_{i,j}^{(g)} & \text{if } j = K \text{ or } \text{rand}_{i,j} [0, 1] \leq Cr \\ x_{i,j}^{(g)} & \text{otherwise} \end{cases} \quad (9)$$

where  $K$  is a randomly chosen integer number in  $\{1, 2, \dots, 2k\}$ ,  $Cr$  is pre-fixed crossover rate. Therefore,  $U_i^{(g)}$  can get at least one component from  $V_i^{(g)}$ .

Step 4.4: Selection

Selection operation selects target or trial vector to survive to the next generation  $g=g+1$ , which can be described as:

$$x_i^{(g+1)} = \begin{cases} U_i^{(g)} & \text{if } f(U_i^{(g)}) \leq f(x_i^{(g)}) \\ x_i^{(g)} & \text{otherwise} \end{cases} \quad (10)$$

where  $f(\cdot)$  is the fitness function defined as:

$$f(X) = \alpha \eta_1(X) + (1 - \alpha) \eta_2(X) \quad (11)$$

where  $\eta_1 = \sum_{\lambda=\lambda_{min}}^{\lambda_{max}} (S_f(\lambda, X) - \Phi(\lambda))^2$ ,  $\eta_2 = \sum_{i=1}^n (e_i - \bar{e})^2 / n$ ,  $e_i = \sum_{\lambda=\lambda_i}^{\lambda_i+\Delta\lambda_i} (S_f(\lambda, X) - \Phi(\lambda))^2$ ,  $\bar{e} = \sum_{i=1}^n e_i / n$ . where  $\eta_1$  denotes sum of squared error (SSE), and  $\eta_2$  is the variance of error distribution which is used to evaluate uniformity of error distribution in the wavelength bands.  $\alpha$  is scale coefficient ranging  $[0, 1]$ , which determines fitness function tended to error value or uniformity of error distribution.  $n$  is the number of wavelength band.

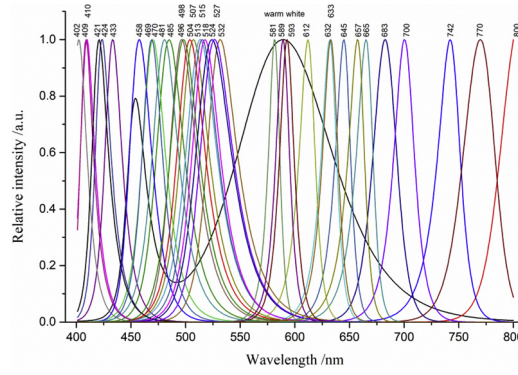


Fig. 2. LED types candidate in range of 400–800 nm for selection in our work.

Iteration operation of steps 4.2–4.4 described above is continued until parameter vector converged or iteration number terminated. Then the best parameter vector  $\mathbf{X}$  is obtained.

Step5: Termination criterion.

Spectral match can then be calculated for  $k$ -types synthesis under parameter vector  $\mathbf{X}$ . Steps 2–4 are repeated until the spectral match deviation reaches design target  $T_{sm}$  or selected type number exceeds total number of candidate LED types  $N$ . Finally, the LED types, number and driving current for each type, spectral match deviation, and synthesized spectrum are recorded as the optimized results output.

## 4. Results and discussion

### 4.1. SPD modeling for the candidate of LED

For work parameters optimization of each type LED, DE algorithm searches current and number to calculate the synthesized spectrum. Therefore, SPD modeling for each type of LED is essential for implementation of SMREA.

The operation of LEDs is determined by three tightly coupled domains: electrical, thermal, and optical domain. To obtain SPD of LED at different operational condition, an experimental platform was developed in our work. LEDs (Szealand photoelectric, China) of 36 types in the range of 400–800 nm shown in Fig. 2 were collected in our work as candidate for AM1.5 G solar spectral synthesis. Integrating sphere (LED7F98, Everfine, China) and fiber optics spectrometer (HR4000, Oceanoptics, USA) were assembled to measure SPD of LEDs. The self-designed program-controlled current sources with resolution of 10 mA were used to provide adjustable drive currents for LEDs. A peltiercooled, temperature controlled cold-plate was used to provide the reference temperature during measurement. The tested LED was attached to cold plate. Therefore, different operational conditions can be set and corresponding SPD data can be measured for modeling and evaluation. In our experiment, the same reference temperature of 20 °C was applied to maintain the consistency of measured spectral data.

Various mathematical spectrum models have been proposed to numerically express SPD such as Gaussian function [25], Lorentz function [26], logistic power peak function [27] and so on. In our work, two-dimensional density of states function described in Eq. (12) and (13) was applied to fit asymmetric SPD of LED [28] for its ability to accurately reflect LED nonlinear spectral features including peak wavelength, full width at half maximum, red shift *etc.*

$$S(\lambda) = \frac{A_m}{\left(1 + \exp\left(-\frac{\lambda - \lambda_{m,c1}}{\omega_{m,1}}\right)\right)\left(1 + \exp\left(\frac{\lambda - \lambda_{m,c2}}{\omega_{m,2}}\right)\right)} \quad (12)$$

$$S(\lambda) = \frac{A_w}{\left(1 + \exp\left(-\frac{\lambda - \lambda_{w,c1}}{\omega_{w,1}}\right)\right)\left(1 + \exp\left(\frac{\lambda - \lambda_{w,c2}}{\omega_{w,2}}\right)\right)} + \frac{A'_w}{\left(1 + \exp\left(-\frac{\lambda - \lambda_{w,c3}}{\omega_{w,3}}\right)\right)\left(1 + \exp\left(\frac{\lambda - \lambda_{w,c4}}{\omega_{w,4}}\right)\right)} \quad (13)$$

where  $S(\lambda)$  denotes SPD,  $A_m$ ,  $\lambda_{m,c1}$ ,  $\lambda_{m,c2}$ ,  $\omega_{m,1}$ ,  $\omega_{m,2}$  are fitted parameters for monochromatic LED. And  $A_w$ ,  $A'_w$ ,  $\lambda_{w,c1}$ ,  $\lambda_{w,c2}$ ,  $\omega_{w,1}$ ,  $\omega_{w,2}$ ,  $\lambda_{w,c3}$ ,  $\lambda_{w,c4}$ ,  $\omega_{w,3}$ ,  $\omega_{w,4}$  are fitted parameters for white LED.

The non-linear curve fit of SPD was performed by Levenberg-Marquardt algorithm. Due to coupling influence of multiple parameters, parameter  $A$  was firstly constrained according to peak wavelength intensity of SPD. Then relation of each parameter of fitted function  $p$  and forward current  $I_f$  was investigated using the non-linear expressions shown in Eq. (14).

$$p(I_f) = \frac{d_1 I_f^2 + d_2 I_f + d_3}{1 - d_0 I_f} \quad (14)$$

where  $p$  denotes the fitted parameters in Eq. (10) and (11),  $d_0$ ,  $d_1$ ,  $d_2$ ,  $d_3$  are the fitted coefficients.

In this way, SPD modeling was established to analytically express the dependence of SPD on forward current. To demonstrate the

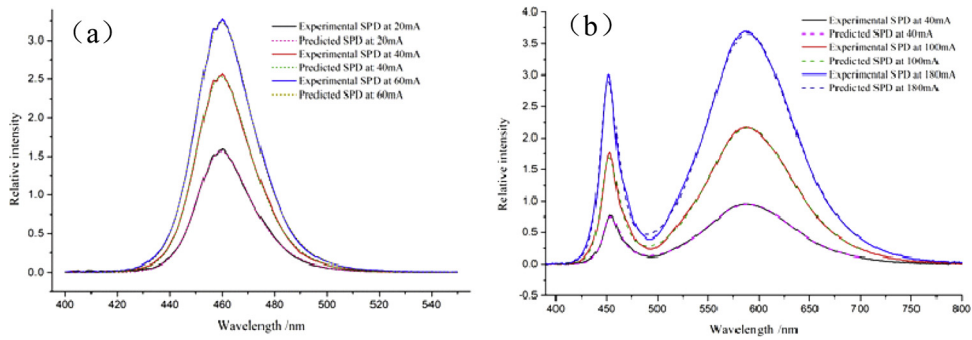


Fig. 3. Comparison of predicted and experimental SPD at different current (a) monochromatic (b) warm white.

effectiveness of SPD model, Fig. 3 illustrates the comparison of the predicted SPD using SPD model and measured result at the different currents for monochromatic and warm white LED respectively. Obviously, the predicted SPDs are in good agreement with the experimental results. It provides an effective method for the optimized computation of multi-LED spectral synthesis.

#### 4.2. Dependence of AM1.5 G solar spectral synthesis on LED type number

SMREA was performed in our work from candidate LED of 36 types to synthesize AM1.5 G spectrum with radiant flux of 10 W in the range of 400–800 nm. During implementation of SMREA, parameters were set as  $\lambda_{min} = 400$  nm,  $\lambda_{max} = 800$  nm,  $\phi\lambda = 20$  nm,  $F = 0.8$ ,  $Cr = 0.2$ ,  $\alpha = 0.6$ . In initial stage  $k = 0$ , warm white LED was selected for prior knowledge of wide spectral range and high power output to contribute spectral synthesis, and then  $k = 1$ .

To systematically analyze the relation between spectral synthesis performance and number of LED types, program was developed to evolve until selected type number exceeds total number of candidate LED types. Synthesized spectrum and optimized working parameters at each generation were saved for analysis. Fig. 4 gives the curve of SSE with LED type number increasing which validates the convergence of algorithm.

The dependence of AM1.5 G solar spectral match degree on LED type number is illustrated in Fig. 5. Spectral match deviation decreases firstly, then fluctuates up and down near a certain value with increment of LED types number. At the initial stage, the increase of LED type has greater improvement for spectral match deviation. But after a certain amount, addition of LED types makes little difference. The result indicates that four types of LED can achieve spectral match deviation 21.45%, which is less than  $\pm 25\%$  and can be rated as Class A level in the range of 400 nm–800 nm. When the number of LED types added to 7 and 11, the spectral match deviation can decreased to be 5.94% and 2.65% respectively. The minimum spectral match deviation can reduced to 0.24% when the combination number of LED types is 23. After evolution arrived 11 types of LED, spectral match deviation changes little and fluctuates around 2%. The evolution process of 11 types is detailed given in Table 1.

At different stage of evolution, increase one type of LED will have different contribution for spectral match reduction. Due to narrow band distribution of monochromatic LED, adding one type of LED will increase the energy ratio of wavelength band where main power of LED located. The spectral match may consequently improve, may go even bad because spectral match defined in the IEC 60904-9 standard relates with the energy ratio of different wavelength band. The retrogress phenomenon encountered at the evolution stage as shown in Fig. 5 and Table 1. Combination of 7 types LED will produce maximum residual at wavelength band of 420 nm–440 nm. After addition of LED type of 433 nm, energy ratio of 400–500 nm increases but the spectral match deviation deteriorates from 5.94% to 6.12%. The similar phenomenon has also occurred in evolutionary stage from 9 types to 10 types. Addition of 507 nm LED causes decrement of energy ratio in 600–700 nm and spectral match deviation retrogress from 5.59% to 7.84%. Certainly, keeping addition of LED type will re-improve spectral match result until it stays stable.

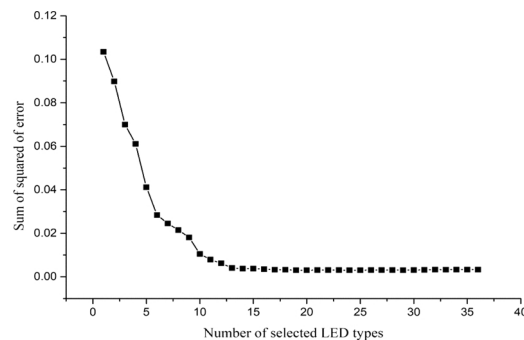


Fig. 4. Relationship of SSE and number of selected LED types.



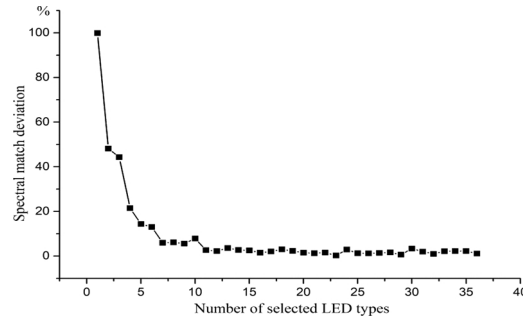


Fig. 5. Dependence of spectral match deviation on number of selected LED types.

Table 1

Detailed SMSEA results of first 11 types.

Generation	LED type selected by SMSEA	400-500	500-600	600-700	700-800	$\sigma_{\lambda-R_{max}}$	Spectral match deviation (%)
1	warm white	0.007089	0.016375	0.013129	0.001192	780-800	99.88
2	800	0.648434	1.481427	1.186691	0.542184	740-760	48.14
3	742	0.556946	1.273064	1.034085	1.099634	400-420	44.31
4	410	0.785503	1.190334	0.967176	1.033057	480-500	21.45
5	485	1.051464	1.125758	0.856727	0.954249	680-700	14.33
6	683	0.980054	1.02726	1.096233	0.869849	700-720	13.02
7	700	0.957714	1.00384	1.05944	0.96987	420-440	5.94
8	433	1.061169	0.962246	1.022289	0.953454	760-780	6.12
9	770	1.041188	0.944123	1.00023	1.026054	500-520	5.59
10	507	1.032591	1.058519	0.921617	0.983323	640-660	7.84
11	645	1.016209	1.020593	0.985019	0.973502	660-680	2.65

Typical selecting and adding process of spectral match residual-guided evolution from 1 types to 4 types and 7 types to 10 types were given in Fig. 6(a)–(d) and (e)–(h) respectively. During evolution, selected LED was marked and it clearly shows the dynamic process of evolution of LED type selection.

Evaluation parameter of spectral match in photovoltaic field reflects the energy ratio of 100 nm wavelength band, and cannot directly reveal multi-LED spectral fitted performance. Figs. 5 and 6 show that increase of LED type cannot continuously improve spectral match, but synthesized spectral distribution become more and more similar with target spectrum. Therefore, correlation index  $R^2$  defined in Ref [20] is introduced in our work to evaluate spectral similarity of multi-LED synthesized and target spectrum.

$$R^2 = 1 - \frac{\sum (S(\lambda) - \Phi(\lambda))^2}{\sum S(\lambda)^2 - (\sum S(\lambda))^2/n} \quad (15)$$

where  $S(\lambda)$ ,  $\Phi(\lambda)$  is the synthesized and targeted spectrum respectively.  $n$  is number of wavelength considered in the spectral range of 400 nm–800 nm. In our work, wavelength interval is 1 nm and then  $n = 400$ .

The spectral match residual-guided evolutionary process also gives the dependence of  $R^2$  on LED type number as shown in Fig. 7. Adding LED types one by one will increase  $R^2$  dramatically at the initial stage and combination of the selected 13 types LED can achieved  $R^2 = 0.984$ . After that, addition of LED types has little improvement of  $R^2$ . Similar results using other selection scheme have been reported in literatures [28]. The changing curve of SSE with number of LED type combination shown in Fig. 4 reveals the same

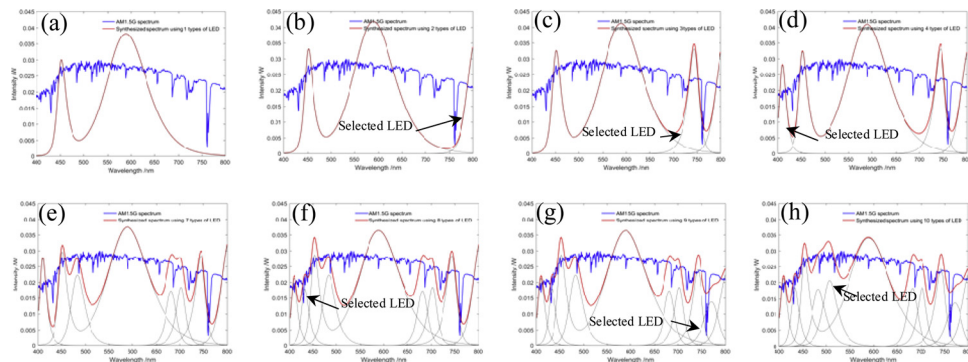


Fig. 6. Typical selecting and adding process of spectral match residual-guided evolution.

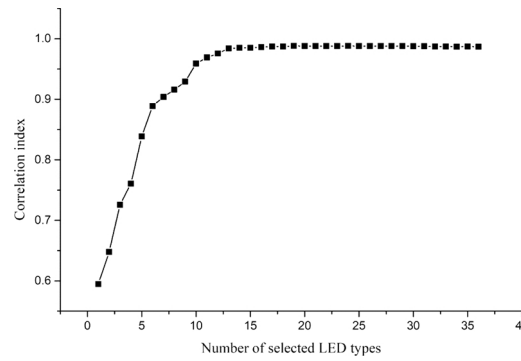


Fig. 7. Dependence of correlation index on number of selected LED types.

trend. After the number reaches 13, SSE has hardly changed at all.

Fig. 8 demonstrates the comparison of AM1.5 G solar spectrum and typical spectral synthesized results at different number of LED types selected by SMREA. Fig. 8(b) indicates that under combination of 13 types, similar wave trough with targeted spectrum around 518 nm, 655 nm, 687 nm, 718 nm, 761 nm have been formed. There are still some large differences in some band such as in the range of 400 nm–405 nm, 415 nm–425 nm, 460 nm–475 nm, 610 nm–640 nm. When the type combination evolved to 19, distinct spectral difference disappears and it reaches maximum  $R^2 = 0.9882$  as show in Fig. 8(c). Consequent addition of LED type will subtly improve spectral shape as illustrated in Fig. 8(d)–(f). It is necessary to note that there are only 2 types of LEDs between 700 nm and 800 nm as candidate in our database, therefore, after evolution to 9 types combination with the two types added, spectral shape in the wavelength band keeps nearly stable and slightly larger deviation of spectral shape still exists. In the spectral range with various types of candidate LED of 400–433 nm and 458 nm–532 nm as shown in Fig. 2, synthesized spectrum coincides better with targeted spectrum after types selection evolved to 19.

Figs. 6 and 8 roughly exhibit the whole evolutionary process of LED-based spectral synthesis at different number of LED types using SMREA. Meanwhile, the corresponding working parameters of LED at different evolutionary stage can be outputted and the results of several typical combinations can be found in Table 2. The results show that SMREA can effectively solve the problems of LED types selection and working parameters optimization for multi-LED AM1.5 G solar spectral synthesis.

The above discussion indicates that spectral match deviation or correlation index of multi-LED spectral synthesis doesn't increase linearly with number of LED types increasing. SMREA reveals that LED type number is not the more, the better. The continuous addition after a certain number makes little to improve design requirement, instead, the design complexity and manufacturing cost is increased. Therefore, modeling and optimization of LED type selection plays an important role for design of multi-LED spectral synthesis application.

## 5. Conclusion

In this paper, spectral match residual-guided evolution algorithm (SMREA) was proposed for LED type selection of LEDs-based AM1.5 G solar spectrum synthesis. Dual optimization of minimum type numbers combination and working parameters of LED for

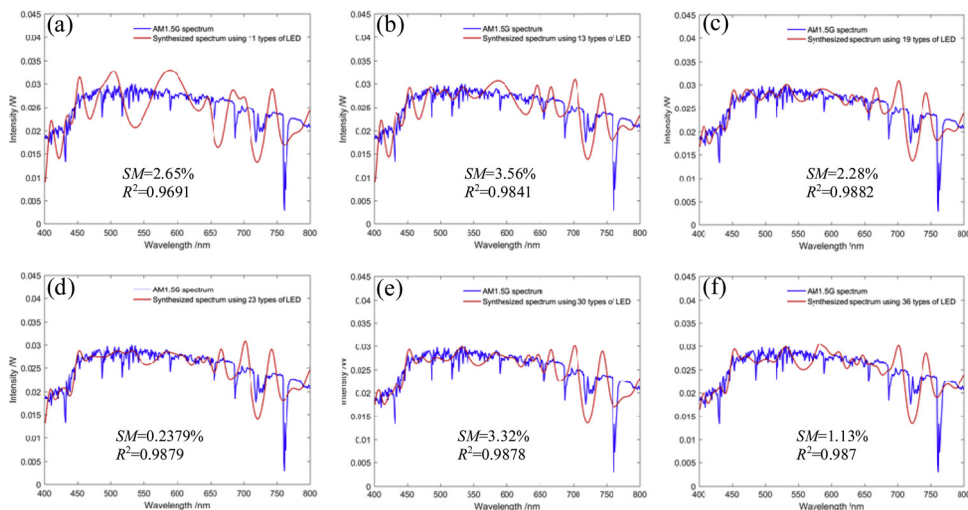


Fig. 8. Spectral synthesized result with different number of LED types selected by SMREA.



**Table 2**  
Optimized working parameters of LED at different number of type combination.

Type of LED	4 types		7 types		11 types		13 types		19 types		23 types	
	$SM = 21.45\%$ $R^2 = 0.7606$		$SM = 5.94\%$ $R^2 = 0.9039$		$SM = 2.65\%$ $R^2 = 0.9691$		$SM = 3.56\%$ $R^2 = 0.9841$		$SM = 2.28\%$ $R^2 = 0.9882$		$SM = 0.238\%$ $R^2 = 0.9879$	
	$I(\text{mA})$	$N$	$I(\text{mA})$	$N$	$I(\text{mA})$	$N$	$I(\text{mA})$	$N$	$II(\text{mA})$	$N$	$I(\text{mA})$	$N$
Warm white	64	10	161	4	56	9	50	9	159	3	154	3
800	55	6	55	6	38	6	27	8	32	7	33	7
742	55	5	60	4	31	6	17	10	25	7	18	10
410	50	3	49	3	60	2	60	2	17	2	22	2
485			60	10	60	8	60	10	32	7	29	8
683			21	10	22	10	13	10	16	9	13	10
700			60	3	60	3	60	4	59	4	60	4
433					34	2	36	2	18	2	36	1
770					60	2	47	3	45	3	45	3
507					60	7	20	9	56	6	28	1
645					60	1	31	2	52	1	53	1
665							40	2	40	2	41	2
532							21	9	20	10	14	10
470									24	3	39	2
409									10	1	14	1
632									20	1	20	1
424									53	1	54	1
612									13	1	22	1
402									40	4	33	3
496											12	3
581											11	2
513											53	6
515											14	1

design objective of spectral match was modeled. To obtain computation model for searching algorithm, SPD modeling was performed for each type LED to numerically express the SPD behavior at different current. Under constraint of 36 LED types database collected in our work, the dependence of spectral match deviation and correlation index on LED type number was systematically investigated by SMREA. The results indicate that performance of spectral synthesis doesn't continuously improve with LED type number increasing. After combination reached a certain number, increasing numbers has little improvement on synthesized spectral performance. In our study, 4 types of LED can achieve spectral match deviation 21.45% of class A spectral match in the range of 400 nm–800 nm with low correlation index 0.7606. When the number of LED types added to 7, 11, and 13, the spectral match deviation can decreased to be 5.94%, 2.65%, 3.65% respectively and the correlation index increases to be 0.9039, 0.9691, 0.9841. Taking performance and cost into account, the best choice of LED type number for AM1.5 G solar spectral synthesis may be 11–13. SMREA can also output working parameters of LED at different evolutionary stage. The feasibility of SMREA to solve the dual optimization problem was effectively validated. The reported work in the paper can provide significant reference for early design of LED-based solar simulator. Certainly, the method is also adaptable for design of LED-based spectrally tunable light source.

## Acknowledgments

This work was supported by National Key Scientific Instrument and Equipment Development Project of China (No. 61427808), NSFC-Zhejiang joint fund for integration of informatization and industrialization (U1609218), Public Projects of the Department of Science and Technology of Zhejiang Province, China (LGG18F050002, LGG18E050005).

## References

- [1] L. Partain, *Solar Cell Device Physics*, Academic Press, 1981.
- [2] V. Esen, Ş. Sağlam, B. Oral, Light sources of solar simulators for photovoltaic devices: a review, *Renew. Sustain. Energy Rev.* 77 (2017) 1240–1250.
- [3] Y. Pan, B. Tao, L. Hang, Study on AM1.5 filter in solar simulator for photovoltaic module solar simulator, *Infrared Laser Eng.* 41 (9) (2012) 2484–2488.
- [4] K. Rühle, M.K. Juhl, M.D. Abbott, et al., Evaluating crystalline silicon solar cells at low light intensities using intensity-dependent analysis of I–V parameters, *IEEE J. Photovolt.* 5 (3) (2015) 926–931.
- [5] A.D. Almeida, B. Santos, B. Paolo, et al., Solid state lighting review – potential and challenges in Europe, *Renew. Sustain. Energy Rev.* 34 (34) (2014) 30–48.
- [6] T. Pulli, T. Dönsberg, T. Poikonen, et al., Advantages of white LED lamps and new detector technology in photometry, *Light Sci. Appl.* 4 (9) (2016) e332.
- [7] M. Bliss, F. Plyta, T.R. Betts, et al., LEDs based characterisation of photovoltaic devices, *International Conference on Energy E-Cient LED Lighting and Solar PhotoVoltaic Systems Conference* (2014).
- [8] S. Kohraku, K. Kurokawa, New methods for solar cells measurement by led solar simulator, *Proceeding of 3rd World Conference on Photovoltaic Energy Conversion* (2003).
- [9] S. Kohraku, K. Kurokawa, A fundamental experiment for discrete-wavelength LED solar simulator, *Sol. Energy Mater. Sol. Cells* 90 (18–19) (2006) 3361–3370.
- [10] M. Bliss, T.R. Betts, R. Gottschalg, Advantages in using LEDs as the main light source in solar simulators for measuring PV devices characteristics, *Proc SPIE: Reliable Photovoltaic Cells, Modules, Components System*, (2008).

- [11] M. Bliss, T.R. Betts, R. Gottschalg, An led-based photovoltaic measurement system with variable spectrum and flash speed, *Sol. Energy Mater. Sol. Cells* 93 (6) (2009) 825–830.
- [12] F.C. Krebs, K.Q. Sylvester-Hvid, M. Jergensen, A self-calibrating LED-based solar simulator test platform, *Prog. Photovolt: Res. Appl.* 19 (1) (2010) 97–112.
- [13] A.M. Bazzi, Z. Klein, M. Sweeney, et al., Solid-state solar simulator, *IEEE Trans. Ind. Appl.* 48 (4) (2012) 1195–1202.
- [14] F. Plyta, T.R. Betts, R. Gottschalg, Towards a fully LED-based solar simulator-spectral mismatch considerations, *Proceedings of the 28th European Photovoltaic Solar Energy Conference and Exhibition* (2013) 3496–3499.
- [15] A. Novičkovas, A. Baguckis, A. Vaitkūnas, et al., Investigation of solar simulator based on high-power light-emitting diodes, *Lith. J. Phys.* 54 (2) (2014).
- [16] A. Novičkovas, A. Baguckis, A. Mekys, et al., Compact light-emitting diode-based AAA class solar simulator: design and application peculiarities, *IEEE J. Photovolt.* 5 (4) (2015) 1137–1142.
- [17] M. Stuckelberger, B. Perruche, M. Bonnet-Eymard, et al., Class AAA LED-based solar simulator for steady-state measurements and light soaking, *IEEE J. Photovolt.* 4 (5) (2014) 1282–1287.
- [18] C.C. Wu, N.C. Hu, Y.C. Fong, et al., Optimal pruning for selecting LEDs to synthesize tunable illumination spectra, *Light. Res. Technol.* 44 (4) (2012) 484–497.
- [19] N.C. Hu, C.C. Wu, S.F. Chen, et al., Implementing dynamic daylight spectra with light-emitting diodes, *Appl. Optics* 47 (19) (2008) 3423–3432.
- [20] H.Y. Yu, G.Y. Cao, J.H. Zhang, et al., Solar spectrum matching with white OLED and monochromatic LEDs, *Appl. Optics* 57 (10) (2018) 2659.
- [21] Photovoltaic Devices—Part 9: Solar Simulator Performance Requirements, IEC 60904-9 Ed.2.0, 2007.
- [22] R.M. Keith, D.A. Malcolm, C.B. Simeon, R. Vishwanath, K. Dieter, M.S. Daniel, Spectral mismatch in modern solar simulators, *29th European Photovoltaic Solar Energy Conference and Exhibition*, (2014).
- [23] R. Storn, K. Price, Differential evolution—a simple and efficient heuristic for global optimization over continuous spaces, *J. Global Optim.* 11 (4) (1997) 341–359.
- [24] A.N. Chalmers, S. Soltic, Light source optimization: spectral design and simulation of four-band white-light sources, *Opt. Eng.* 51 (4) (2012) 044003.
- [25] Y. Uchida, T. Taguchi, Lighting theory and luminous characteristics of white light-emitting diodes, *Opt. Eng.* 44 (4) (2005) 16–34.
- [26] J. Fan, M.G. Mohamed, C. Qian, Color shift failure prediction for phosphor-converted white LEDs by modeling features of spectral power distribution with a nonlinear filter approach, *Materials* 10 (7) (2017) 819.
- [27] F. Reifegerste, J. Lienig, Modelling of the temperature and current dependence of LED spectra, *J. Light. Vis. Environ.* 32 (3) (2008) 288.
- [28] G.Q. Xu, J.H. Zhang, G.Y. Cao, Solar spectrum matching using monochromatic LEDs, *Light. Res. Technol.* 249 (4) (2017) 497–507.